Thermal Conductivity in Ferromagnetic Materials using Molecular Dynamics Simulations

Anthony Lonsdale

Advisor: Dr. Aleksandr Chernatynskiy,

Physics Department

April 1st, 2021

Abstract Insulating non-magnetic solids conduct heat through the lattice vibrations, also colloquially known as phonons. In magnetic solids, additional channels for heat transport are available through the interaction of magnetic moments. Opposing this interaction are lattice vibrations which couple with the magnetic moments on the atoms and thus provide additional resistance to heat flow. There is currently no complete understanding of the magnitudes of these contributions, and the overall effect of the magnetic contribution is largely unknown. Using a combination of spin dynamics and molecular dynamics simulations, we modeled the contribution of the magnetic subsystem to the lattice thermal conductivity across ferromagnetic to paramagnetic transitions in elemental Iron. Application of the approach to the anti-ferromagnetic materials is discussed for the example of the technologically important material, uranium dioxide.

Introduction Pressed uranium dioxide (UO_2) pellets are used in the nuclear fuel rods in over 90% of nuclear fission reactors on the planet, covering roughly 14% of global electricity consumption [1]. These fuel rods, which are organized into fuel assemblies, are specifically designed to allow optimal heat transfer to the water surrounding the fuel assembly during reactor operation. One of the limiting factors of fuel assembly design is the thermal conductivity constant of UO2, which can be calculated using Fourier's law of thermal conduction, $J_z = -k_z \frac{dT}{dz}$, where J_z, k_z and $\frac{dT}{dz}$ represent z-direction heat flux, thermal conductivity, and temperature gradient, respectively.

If the thermal conductivity of UO_2 is lower than expected, then the cores of each fuel pellets may overheat, requiring a smaller diameter fuel pellet for safe operation, with the opposite being true if thermal conductivity is larger than expected. Thermal conductivity in cubic fluorite structures is presumed to be isotropic (symmetric) due to its symmetric structure. Prior experimental results show anisotropic thermal conductivity for UO_2, which suggests that there is a directional dependence for the value of thermal conductivity [2]. These results were supported by molecular dynamics (MD) simulations using classical interatomic potentials, which are infeasible due to the lack of magnetic interaction present in the interatomic potential used. MD simulations which we reproduced using these classical interatomic potentials showed a magnitude of anisotropy of 0.04%, compared to 14.2% as measured by Gofryk et al. A possible explanation for this discrepancy is due to UO_2's anti-ferromagnetic properties at very low temperatures.

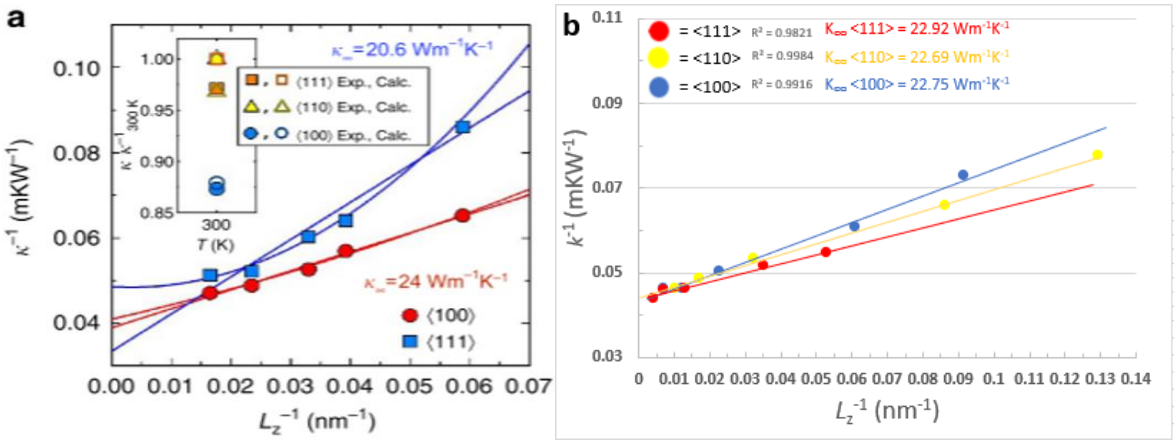

Figure 1 | Anisotropic and Isotropic UO_2 thermal conductivity from MD simulations. The thermal conductivity (k) variation (k^{-1}) as a function of the length of the simulation cell (L_z^{-1}) for the temperature gradient applied in the <100> <110> and <111> lattice directions at 300K. (a) Inset from Gofryk et al compares the experimentally measured thermal conductivity values in the <100> and <111> lattice directions from the non-equilibrium MD simulations [1]. Trendlines indicate linear and quadratic fits used for extrapolation to infinite length simulation cells (K_∞). (b) Inset compares the experimentally measured thermal conductivity values in the <100> <110> and <111> lattice directions from the non-equilibrium MD simulations. Trendlines indicate linear fits to the data used for extrapolation to infinite length simulation cells (K_∞).

Recent developments using the LAMMPS spin dynamics (SD) simulation package, in conjunction with MD simulation, allow for the possibility of an accurate determination of UO_2's thermal conductivity properties. The spin structure of UO_2, which previously has not been accounted for, is most closely approximated as anti-ferromagnetic at low temperatures.

Methods MD simulations using classical potentials for UO_2 employed the direct method, in which non-equilibrium MD simulations apply a heat flux across a material, to calculate thermal conductivity using Fourier's law. All calculations were performed with scalable parallel short-range LAMMPS MD code, closely following the study by Watanabe et al [3]. A constant heat flow ranging from 0.5 to 2 eV/ps was applied per time step depending on system size. The length of the rectangular cuboid simulation cell systems varied from 40-500 nm along the <100> <110> and <111> crystallographic directions and consisted of a face-centered cubic (fcc) lattice structure. The time step size was 1.0 fs in all simulations. To equilibrate the thermal properties of the systems, each simulation performed a constant temperature and pressure (NVT) simulation for 10 ps. The heat flow was applied to each simulation for 300ps after the NVT simulation, generating a thermal gradient. A runtime ranging from 300-2000ps (varying based on system size) was needed for the thermal gradient to reach steady state, with the last 300ps of each simulation being used as the data acquisition time. Statistical analysis was used to extrapolate thermal conductivity measurements to a simulation cell of infinite length, where errors of 2.16%, 0.96% and 1.10% were associated with measurements along the <100> <110> and <111> crystallographic directions, respectively [4].

The approach used by Gofryk et al to determine UO_2's thermal conductivity relies on the aforementioned direct method, which used classical potential developed by Basak et al in 2003 [5]. Basak's model employs the following potential formula:

$$V(r_{ij}) = V_{Coul}(r_{ij}) + V_{Buck}(r_{ij}) + V_{Morse}(r_{ij}) \quad (1)$$

where $V(r_{ij})$ is the potential energy of two atoms (i and j) separated by a distance r_{ij}. The first term in the equation defines the long-range electrostatic interaction between the two atoms with charges q_i and q_j (with ϵ_o being the permittivity of free space).

$$V_{Coul}(r_{ij}) = \frac{q_i q_j}{4\pi\epsilon_o r_{ij}} \quad (2)$$

With the Coulomb interaction being accounted for, this leaves the short-range Buckingham and Morse interactions, which are defined as the following:

$$V_{Buck}(r_{ij}) = f_0 b_{ij} \exp\left(\frac{a_{ij} - r_{ij}}{b_{ij}}\right) - \frac{C_{ij}}{r^6{}_{ij}} \tag{3}$$

$$V_{Morse}(r_{ij}) = f_0 d_{ij}\left[\exp\{-2\gamma_{ij}(r_{ij} - r^*{}_{ij})\} - 2\exp\{-\gamma_{ij}(r_{ij} - r^*{}_{ij})\}\right] \tag{4}$$

where the terms f_o, a_{ij}, b_{ij}, C_{ij}, D_{ij}, γ_{ij}, and $r^*{}_{ij}$ specify each pair interaction. The values for each term are given in the following table, taken from Basak's model:

Parameters	O–O	U–U	O–U
a_{ij} /Å	3.82	3.26	3.54
b_{ij} /Å	0.327022	0.327022	0.327022
C_{ij} /eVÅ^6	3.948787	0.0	0.0
d_{ij}/r^*_{ij}	NA	NA	13.6765
γ_{ij}/r^*_{ij}	NA	NA	1.65
r^*_{ij}	NA	NA	2.369
f_0 /eVÅ^{-1}	0.042203	0.042203	0.042203

The purpose of the classical potential used in Basak's model, is to generate accurate positions of atoms and interatomic interactions in a molecular lattice structure, which can then be used in an MD simulation to measure thermal properties. The classical potential's drawback is that it is an approximation, and it fails to capture the influence of a material's spin structure on its thermal properties. This can be rectified with the inclusion of the LAMMPS SPIN package, which allows for the study of the magnetic properties of materials through simulation of atomic magnetic spins coupled to lattice vibrations.

Of the six magnetic interatomic interactions defined by the SPIN package, the exchange interaction between pairs of magnetic spins is given as the following summation over pairs of nearest neighbors:

$$\boldsymbol{H}_{exchange} = -\sum_{i,j,i\neq j}^{N} J(r_{ij})\, \vec{s}_i * \vec{s}_j \tag{5}$$

Where the neighboring magnetic spins of atoms i and j, are represented as unit vectors $\vec{s}_i$ and $\vec{s}_j$, and $r_{ij} = |\vec{r}_i - \vec{r}_j|$ is the interatomic distance between these two atoms. The function $J(r_{ij})$ is a function defining the magnitude and the sign of the exchange interaction for different neighboring shells, with a negative sign simulating an anti-ferromagnetic system, and a positive sign simulating a ferromagnetic system.

From the exchange interaction, each spin i will have a magnetic torque $\vec{\omega}_i$ and a force $\vec{F}_i$ applied for spin-lattice calculations such as the following:

$$\vec{\omega}_i = \frac{1}{\hbar} \sum_{j}^{Neighbor} J(r_{ij})\, \vec{s}_j \;\; and \;\; \vec{F}_i = \sum_{j}^{Neighbor} \frac{\partial J(r_{ij})}{\partial r_{ij}} (\vec{s}_i * \vec{s}_j)\vec{e}_{ij} \qquad (6)$$

With $\hbar$ is Planck's constant and $\vec{e}_{ij} = \frac{\vec{r}_i - \vec{r}_j}{|\vec{r}_i - \vec{r}_j|}$ is the unit vector between neighboring sites i and j.

Using the exchange interaction detailed above allows us to simulate coupled spin dynamics and molecular dynamics as described by Tranchida et al [6]. Due to the present lack of a magnetic description of UO_2, we instead will use Iron as an analogue. Three operations are applied to a box consisting of 10x10x10 iron atoms in a body-centered cubic (bcc) lattice arrangement. The first operation applies a precession torque to each magnetic spin in the group. The second operation accounts for temperature effects from the first operation by connecting the spin i to a thermal bath using a Langevin thermostat. The third and final operation performs a symplectic integration with a microcanonical ensemble (NVE) for the spin-lattice system, accounting for motion effects. Systems ranging from 50-1000 degrees Kelvin were simulated using time steps of 1.0 fs in all simulations. The quantities of the x y and z coordinates of the total magnetization, along with the norm of the total magnetization was gathered from all systems. Magnetization data followed expected behavior ferromagnetic and anti-ferromagnetic behavior, as well as phase transition behavior, as determined by the exchange interactions.

Discussion To determine the contribution of the magnetic subsystem on the lattice thermal conductivity of the iron, a temperature gradient must be induced in the lattice. Fourier's law can then be used to calculate the thermal conductivity constant for the material in question. This can eventually be done with the technologically important material, UO_2, across its anti-ferromagnetic, ferromagnetic, and paramagnetic phases, allowing a proper analysis of the magnetic subsystem's contribution to the thermal conductivity of the material.

The absence of a description for UO_2's magnetic interactions currently prohibits any determination of the contribution of UO_2's magnetic sublattice on its thermal properties. If the magnetic interactions of UO_2 become known in the future, then following the methods laid out above using the coupled spin and molecular dynamics approach can lead to the accurate determination of UO_2's thermal conductivity and of any possible anisotropic behavior.

Results A visual representation of the spin vectors in an Iron (Fe) lattice shows expected ferromagnetic, anti-ferromagnetic behavior at 300 degrees Kelvin, as well as expected paramagnetic behavior at 1000 degrees Kelvin, as shown below:

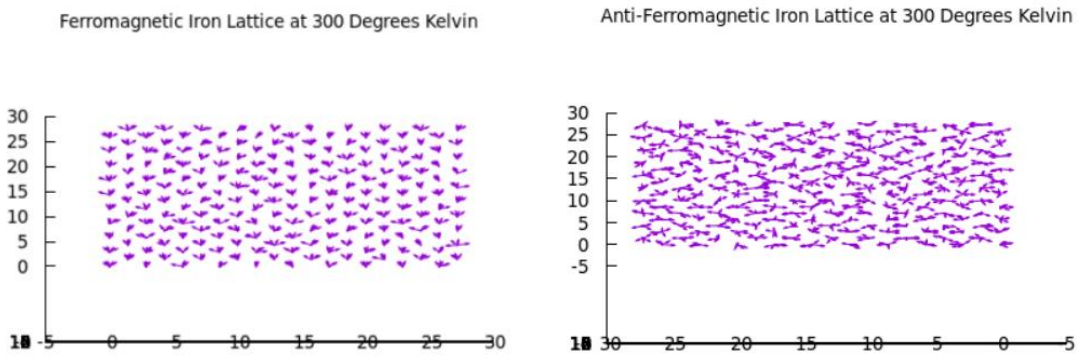

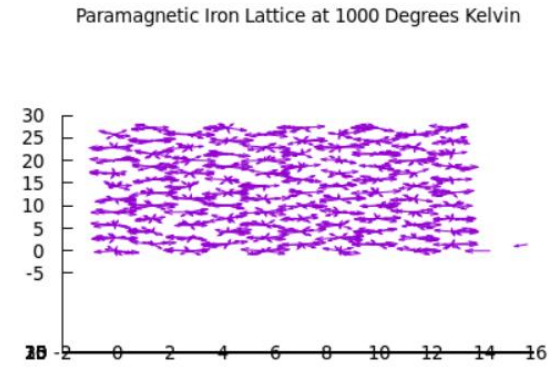

The spins in the ferromagnetic iron lattice are shown to have a clear unidirectional alignment, correlating positively with expectations. The spins in the anti-ferromagnetic iron lattice, show an opposite alignment, correlating positively with expected behavior. Note that the anti-ferromagnetic iron lattice was simulated using a negative exchange interaction and that iron is not anti-ferromagnetic in nature at these temperatures. The spins in the paramagnetic iron lattice show disorder in the spin, again correlating with expected behavior.

Plotting magnetization versus temperature for the ferromagnetic iron lattice sample shows the ferromagnetic to paramagnetic transition occurring as the temperature approaches 1000 degrees Kelvin.

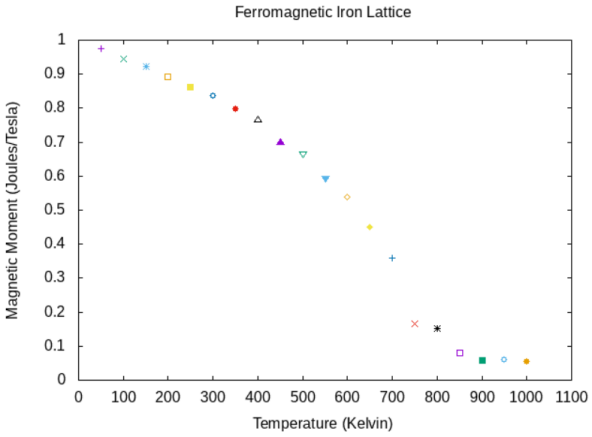

This rapid decrease in magnetization of the iron lattice as the temperature reaches 1000 degrees Kelvin is significant, as it correlates with the Curie point of iron, the point at which magnetization is destroyed due to extreme heat.

Conclusion Now that we understand that the approach using spin and molecular dynamics generates accurate results for the bcc iron lattice system and models the appropriate magnetization behaviors, we have confidence that this approach can be applied to the fcc UO_2 lattice system [7]. Further work is necessary to determine the underlying magnetic interactions of UO_2, once that is complete then it allows for accurate spin and molecular dynamics simulations to be made of the UO_2 species.

Acknowledgements I want to extend my appreciation to my faculty advisor Dr. Aleksandr Chernatynskiy for guiding me through the research process and for being an exceptional teacher.

Project was funded via Missouri S&T's OURE program.

References

1. Wang, Lian & Kaye, M. (2020). Oxide power reactor fuels. 10.1016/B978-0-08-102571-0.00005-7.
2. Gofryk, K., Du, S., Stanek, C. *et al.* Anisotropic thermal conductivity in uranium dioxide. *Nat Commun* **5,** 4551 (2014). https://doi.org/10.1038/ncomms5551
3. Schelling, P.K., Phillpot S.R., and Keblinski, P. Comparison of atomic-level simulation methods for computing thermal conductivity. *Phys. Rev. B* **65,** 144306 – Published 4 April 2002
4. Watanabe, T. *et al.* Thermal transport properties of uranium dioxide by molecular dynamics simulations. *J. Nucl. Mater.* **375,** 388–396 (2008).
5. Basak, C., Sengupta, A. & Kamath, H. Classical molecular dynamics simulation of UO2 to predict thermophysical properties. J. Alloys Compd. **360**, 210–216 (2003)
6. Tranchida, Plimpton, Thibaudeau and Thompson, Journal of Computational Physics, **372**, 406-425, (2018).
7. S. Plimpton, Fast Parallel Algorithms for Short-Range Molecular Dynamics, J Comp Phys, **117**, 1-19 (1995).